SDC-90-00066

PI
T

SDC
SOLENOIDAL DETECTOR NOTES

EFFECTS OF NON-UNIFORM MAGNETIC FIELDS ON SDC CENTRAL TRACKING

John A.J. Matthews

August 1990

Effects of Non-uniform Magnetic Fields on SDC Central Tracking

John A.J. Matthews
Johns Hopkins University
Baltimore, MD 21218

August 1990

1. Introduction

Both long coil and short coil options are being considered for the SDC solenoid. For the long coil the field in the central tracking volume is essentially ideal, and need not be discussed further. However for the short coil option[1] there are substantial radial components in the magnetic field. It is therefore of interest to understand the effect of the short coil magnetic field on the performance of the central tracking systems.

The outline of this note is as follows. In Section 2, we determine the effective magnetic field integral for the short coil field in order to estimate how the reduced field will degrade the momentum resolution of the tracking system. A more subtle effect is the impact of the non-uniform field on the pattern recognition capabilities of the tracking system. This is studied in Section 3 in a model where tracks are identified by the clustering of tracking superlayer measurements in curvature – phi space. In this case the non-uniform magnetic field will spread out the clusters and thus degrade the fast track finding capability of the system. Finally Section 4 provides a summary.

2. The Effective Magnetic Field Integral for the Short Coil

The magnetic field lines for the short coil field are shown in Fig. 1, where field lines are mapped out at 10 cm intervals in radius. Qualitatively the field is worst at large z, and at large r. The main point to be made from this figure is that the bending of a track in the field goes to zero when the track is parallel to the field line; this is close to happening for tracks at the ends of the tracking volume.

To obtain a more quantitative estimate of the effect of the short field consider the net impulse given to a high momentum track traversing the magnetic field:

$$\Delta\vec{p} = -e\int \vec{B} \times \vec{ds}$$

where $\vec{p}$ is the track momentum vector, $\vec{ds}$ is along the track momentum direction, and $\vec{B}$ is the magnetic field. To a first approximation the momentum resolution of a tracking system is proportional to:

$$(\frac{\sigma_p}{p^2}) \propto \frac{1}{|\Delta \overrightarrow{p}|}$$

The value of $|\Delta \overrightarrow{p}|$ for tracks at $\eta = 0$ is essentially the same for a uniform field and for the short coil field; this is not the case for all η values. To illustrate the magnitude of the effect, Fig. 2a-c) shows the dependance of $|\Delta \overrightarrow{p}|$ on η, normalized to the value at $\eta = 0$, for tracking systems that extend radially to 50cm (silicon), 110cm, and 170cm (full tracking system) respectively. The curves look rather similar and show that a degradation in momentum resolution of 10% - 20% is expected near the end of the maximum rapidity range available for tracking.

3. Effects of the Short Coil Field on Pattern Recognition

The proposed tracking systems for the SDC detector are designed with a *superlayer* structure,[2] where a superlayer provides a measurement of the track position, ϕ, and also the local track slope, $(\frac{d\phi}{dr})$, or $(\frac{d\phi}{dz})$. This information is sufficient to estimate the track curvature, and azimuthal angle at the origin, from each superlayer measurement. The approach is as follows.

Tracks starting at the beam line will move in helical paths through the tracking volume:

$$r = 2\rho \; sin(\phi_0 - \phi)$$

$$z = 2\rho(\phi_0 - \phi)tan\lambda \;\; + \;\; z_0$$

where r is the radial distance of the track from the beam line, z is the distance along the beam line from the nominal beam interaction point, z_0 is the actual z location of the interaction point, ϕ is the azimuth of the track at (r, z), ϕ_0 is the initial track azimuth at the origin, ρ is the track radius of curvature in the x, y plane, and $tan\lambda$ is the tangent of the dip angle, λ. Alternatively $tan\lambda$ is given by the cotangent of the angle of the track to the beam direction. It is convenient to define the track curvature, $\kappa \equiv \frac{1}{2\rho}$. Thus κ is related to the magnetic field, B, and the track P_t: $\kappa = \frac{0.3B}{2P_t}$, where κ is in m^{-1}, B is in Tesla, and P_t is in GeV/c. Differentiating the track equations above gives for the central region:

$$\kappa = \frac{-(\frac{d\phi}{dr})}{\sqrt{1 + (r\frac{d\phi}{dr})^2}}$$

and for the forward region:

$$\frac{\kappa}{tan\lambda} = -(\frac{d\phi}{dz})$$

The helix equations can then be inverted to solve for ϕ_0, which for central tracking is given by:

$$\phi_0 = \phi + sin^{-1}(\kappa r)$$

and the analogous relation for forward tracking is given by:

$$\widetilde{\phi_0} \equiv \phi_0 + \frac{\kappa z_0}{tan\lambda} = \phi + z(\frac{d\phi}{dz})$$

Thus each superlayer provides a measurement of (κ, ϕ_0) for the axial detectors in the central tracker, or a measurement of $(\frac{\kappa}{tan\lambda}, \widetilde{\phi_0})$, for the forward silicon planes. Track finding can then be done by searching for clusters of points in $\kappa - \phi_0$ space, and separately in $\frac{\kappa}{tan\lambda} - \widetilde{\phi_0}$ space.

Since this track finding procedure assumes uniform helical motion for a track, it is important to understand the impact of the non-uniform short coil magnetic field. To estimate the effect a simple simulation[3] was done to compare the results obtained when using either an ideal magnetic field, or the short coil field, to track particles through a representative SDC tracking system as sketched in Fig. 3. The tracks were generated at discrete values of P_t, and were distributed uniformly in rapidity. The superlayer hits were then plotted in curvature-phi space. A qualitative impression of the clustering of points for an ideal field, and for the short coil magnetic field, can be obtained from Fig. 4 which shows examples of several $P_t = 1$ GeV/c tracks in the rapidity interval $1.75 < |\eta| < 2.5$ in the forward silicon planes. The visual impression from the few tracks is that the short field effects are somewhat greater than the natural smearing from measurement errors or from multiple scattering.

To be more quantitative Fig. 5 shows the RMS width of the normalized curvature distributions, $\frac{\kappa_{simulation} - \kappa_{true}}{\sigma_\kappa}$, obtained from various Monte Carlo simulations. This is a useful quantity since the expected measurement error, σ_κ, sets the natural scale for deciding which effects are relevant in smearing the curvature distributions. Note, σ_κ is determined separately for each superlayer. The simulation results are divided by detector type: axial silicon, forward silicon planes, and large radius axial tracking systems. Results are given for an ideal magnetic field with and without multiple scattering, for an ideal magnetic field with the initial (x, y) track origin distributed with a Gaussian distribution of widths, $\sigma_x = \sigma_y = 500\mu$-meters, and for the short coil magnetic field with no multiple scattering. With the exception of the x, y vertex smearing, the short coil field results in the greatest spreading of the curvature distribution. Since the effective RMS centroid motion of the beam should be substantially less than 500μ-meters, these simulations indicate that the short coil field is the dominant source of broadening of the curvature-phi track clusters for $P_t < 5$ GeV/c in the $|\eta| > 1$ region for the large radius axial tracking system, and for the $|\eta| > 1.75$ region for the forward silicon planes.

4. Summary

The effect of the short coil magnetic field on track momentum resolution was estimated to represent less than a 20% reduction in the resolution even at the largest rapidities covered by the tracking system. The effect of the short coil magnetic field on fast track finding indicates that at large rapidity, $|\eta| > 1$ for the full tracking system and $|\eta| > 1.75$ for the forward silicon planes, and at low momentum, $P_t < 5$ GeV/c, then the smearing of superlayer points in curvature-phi space is significant. However tracking for $P_t > 5$ GeV/c is unaffected, and tracking for $P_t > 1$ GeV/c is unaffected for central values of rapidity.

5. References

1. The short coil magnetic field was as obtained from B. Wands of Fermilab in May 1990. The parameters of the current sheet were: radius = 2.06 meters, and total length = 9 meters.
2. **The Solenoid Detector Collaboration EOI**, E. Berger etal, May 24, 1990
3. The simulation used the simulation package SILANL: **SILANL - Silicon Tracking System Simulation Program for the SSC**, J. Hylen, J. Matthews, A. Weinstein (1990)

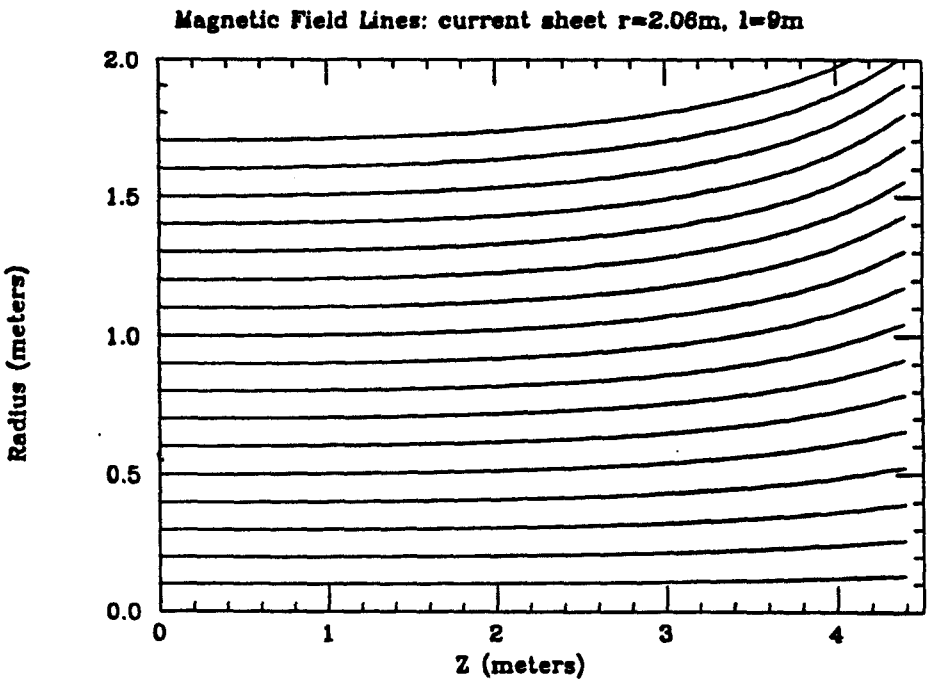

Figure 1 Map of magnetic field lines for the short coil magnetic field. The lines are drawn at 10 cm intervals radially starting from $z = 0$.

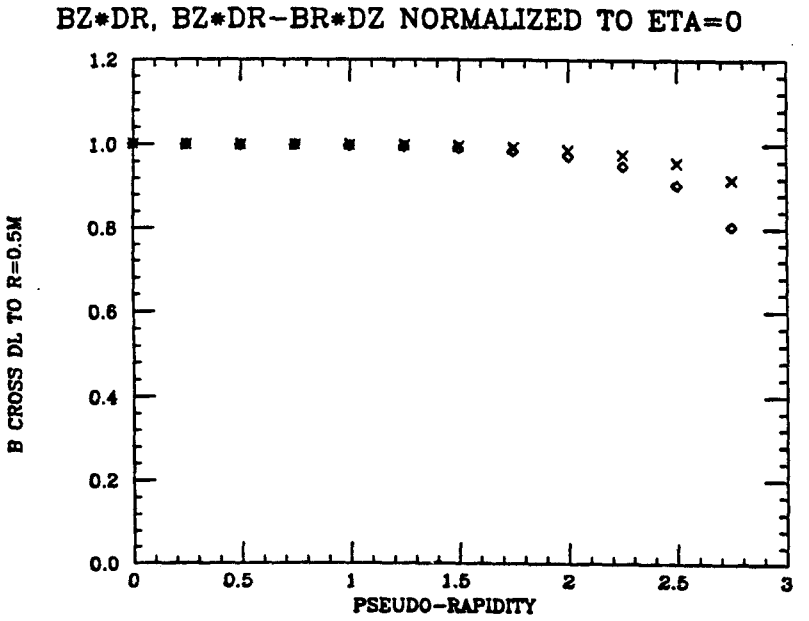

Figure 2a) $\frac{\int B_z dr}{(\int B_z dr)_{\eta=0}}$, denoted by (×), and $\frac{\int \vec{B} \times \vec{ds}}{(\int \vec{B} \times \vec{ds})_{\eta=0}}$, denoted by (◇), as a function of track rapidity. The magnetic field integrals are evaluated out to $r = 0.50$ m, and for $|z| < 4.5$ m.

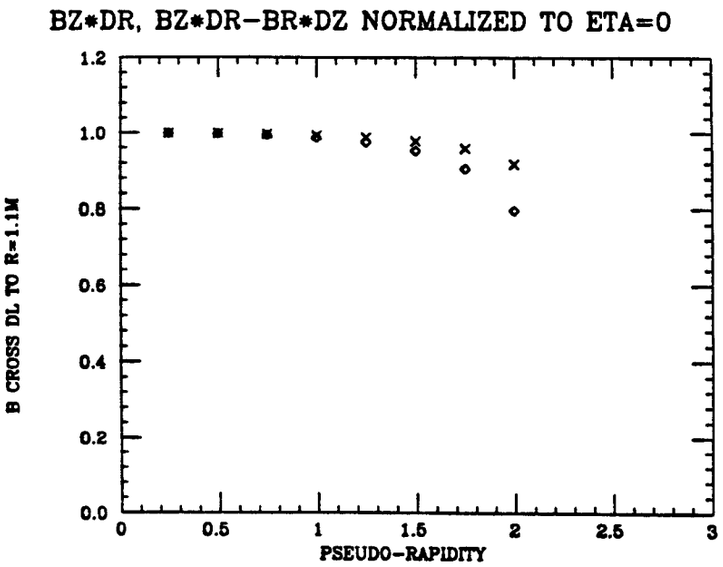

Figure 2*b*) As in Fig.2a) except that the magnetic field integrals are evaluated out to $r = 1.10$ m, and for $|z| < 4.5$ m.

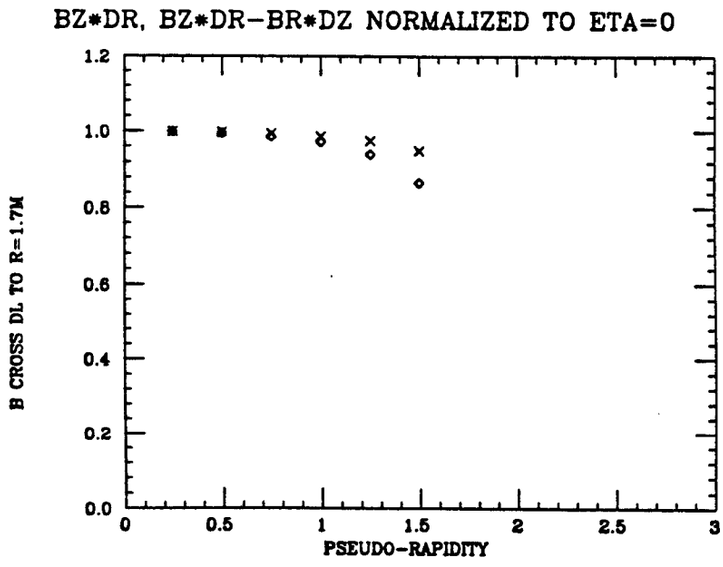

Figure 2*c*) As in Fig.2a) except that the magnetic field integrals are evaluated out to $r = 1.70$ m, and for $|z| < 4.5$ m.

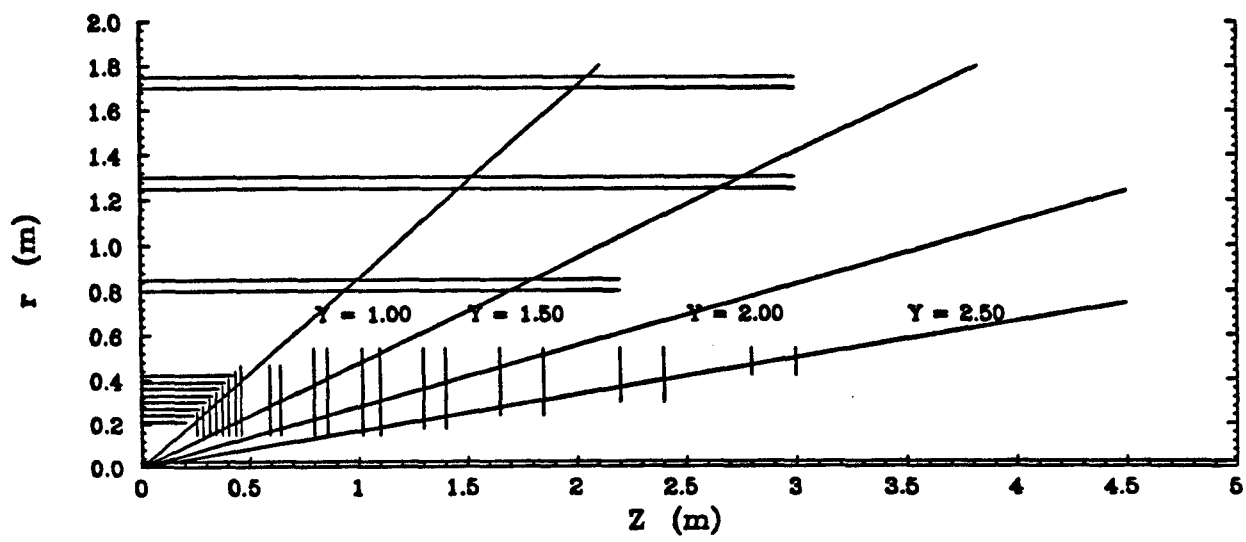

Figure 3 Quarter-section schematic showing a possible SDC tracking system; the lines show various values of rapidity.

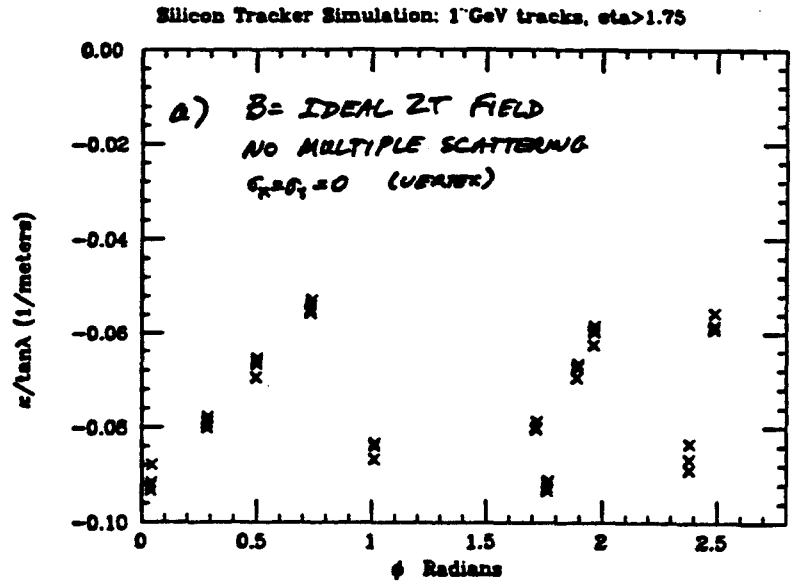

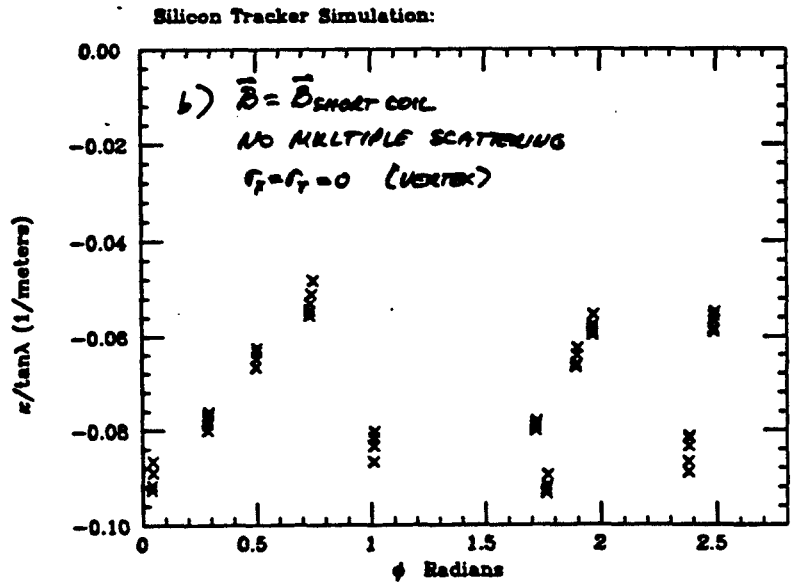

Figure 4 Superlayer measurements of $\frac{\kappa}{tan\lambda}$ versus $\widetilde{\phi_0}$ for P_t =1 GeV/c tracks with $|\eta| > 1.75$ as simulated in the forward silicon planes: a) ideal magnetic field with no multiple scattering, b) short coil magnetic field with no multiple scattering.

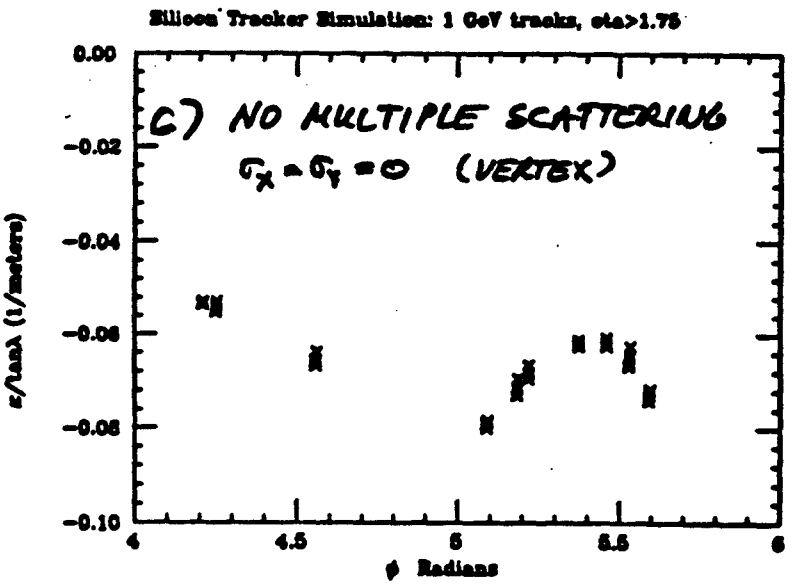

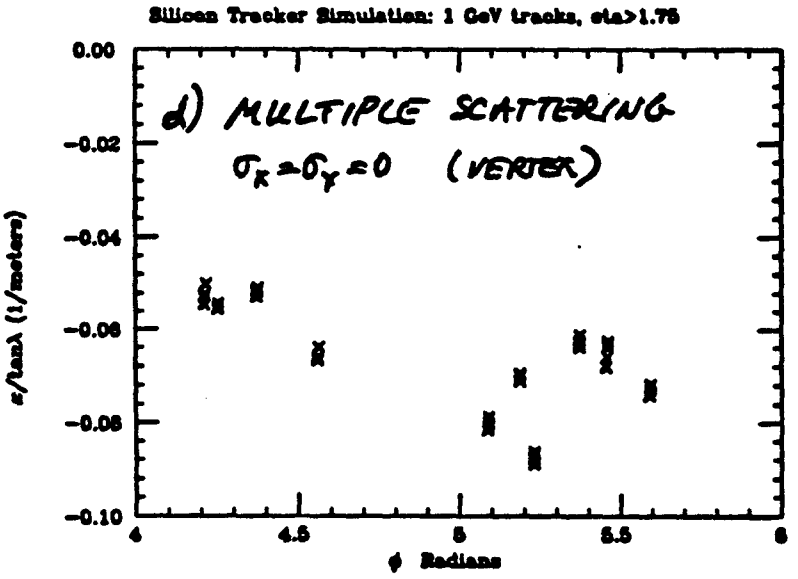

Figure 4 As in Fig.4a,b) with the variations: c) ideal magnetic field with no multiple scattering, d) ideal magnetic field with multiple scattering.

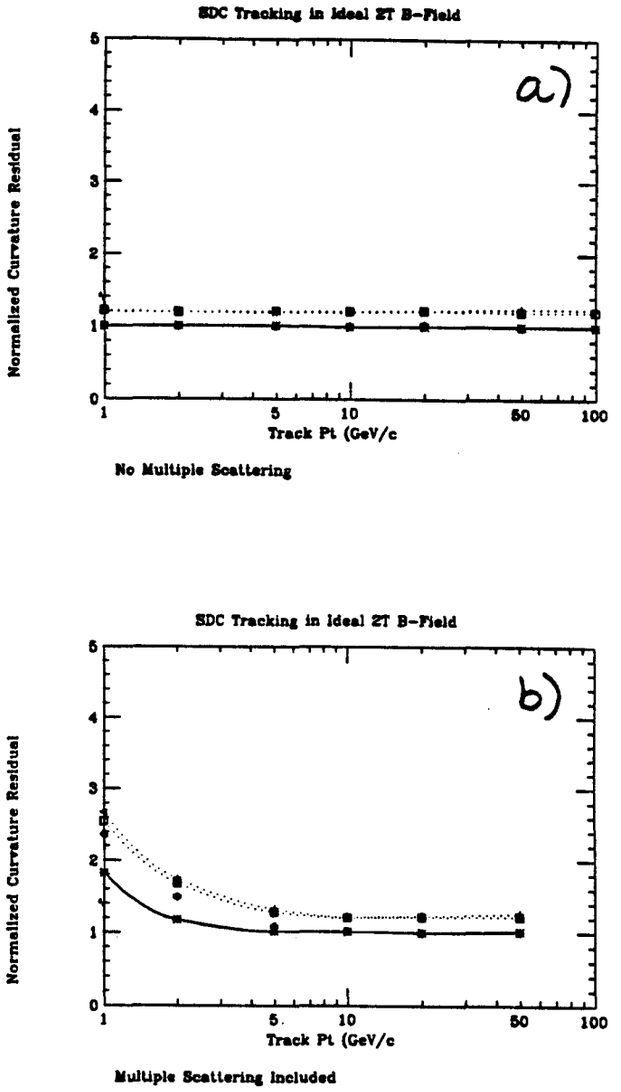

Figure 5 Superlayer measurements of $\frac{\kappa_{simulation}-\kappa_{true}}{\sigma_\kappa}$, shown as a function of track P_t, as simulated in the SDC tracking systems. The dotted line connects the results for the forward silicon planes in the intervals: $1 < |\eta| < 1.75$ and $1.75 < |\eta| < 2.5$; the solid line connects the results for the axial large radius tracking system in the intervals: $0 < |\eta| < 1$ and $1 < |\eta| < 1.75$. The unconnected points are from the axial silicon system, $|\eta| < 1$. Results are shown for: a) ideal magnetic field with no multiple scattering, b) ideal magnetic field with multiple scattering.

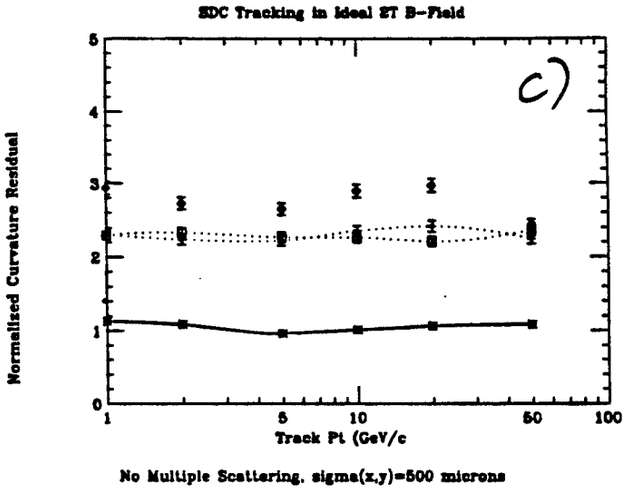

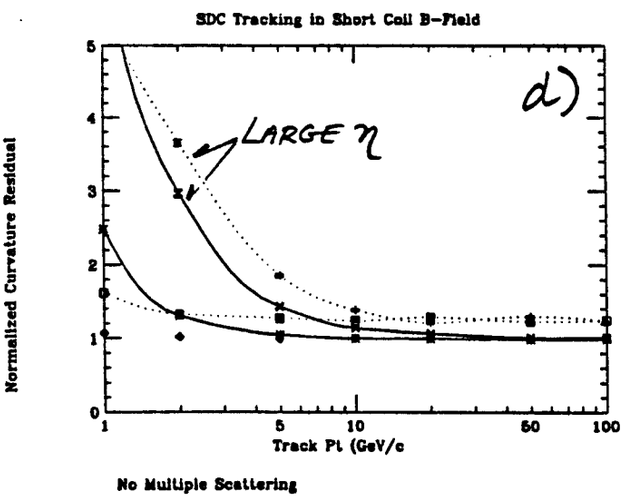

Figure 5 As in Fig.5a,b) with the variations: c) ideal magnetic field, no multiple scattering, and initial track (x, y) distributed with Gaussian widths $\sigma_x = \sigma_y = 500\mu$-meters, and d) short coil magnetic field with no multiple scattering.